Corona in visible light

- F corona: light scattered by interplanetary dust particles
    - unpolarized (within 5-6 R_{Sun})
    - nearly constant in time and unaffected by CME
    - with absorption lines
- K corona: light scattered by electrons in the corona - Thomson scattering
    - polarized radial (CME?) and tangetial (electrons along magnetic loops?) to the solar limb
    - no absorption lines because of high temperatures

The brightness of the K corona falls off much more rapidly with distance from the Sun such that it dominates close to the Sun, is roughly equal to the F corona at $\approx 4\ R_{Sun}$, and is much dimmer than the F corona far from the Sun.

Comparison with LASCO observations

- close to the sun the light is scattered mostly in the plane of sky
- use coronagraph with large field of view LASCO (located on SOHO spacecraft, no atmosphric scattering) for C2 up to 6 R_{Sun} and C3 up to 32 R_{Sun}
- synthetic images created by numerically integrating the Thomson-scattered light along a LOS ($\Longleftarrow$ oplically thin corona) for each pixel with the appropriate scattering function
- make truly quantitative comparisons with the data
- account for F corona far from the Sun, where it is the dominant source of scattered light
- the contribution of dust scattering with the same power-law empirical relationship used to make the LASCO images. In this case, the background F corona brightness is taken to have the form: $B_F = cr^{0.22cos(2\theta)-2.47}$. $c = \{c \mid B_F(r = 4R_{Sun}) = B_k\}$,where B_K is the background polar brightness of the K corona.
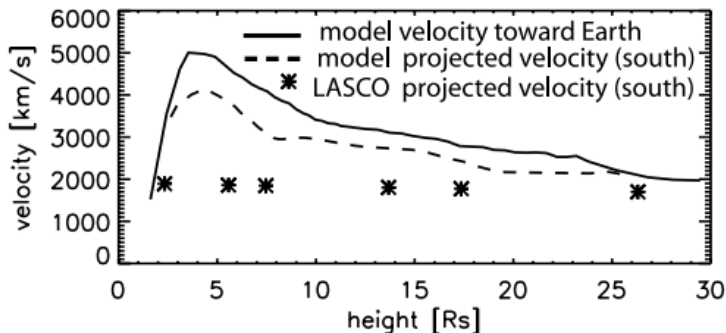
Velocity comparison

Fig. 4.—Comparison of observed and modeled CME velocity. The solid line shows the modeled CME velocity moving directly toward the Earth, while the dashed line shows the model velocity projected on the plane of the sky 177° (counterclockwise) from the north polar axis. At this same location in the plane of the sky, the CME velocity is derived from LASCO observations and plotted with stars. We find that the model briefly reaches a velocity of 4000 km s^{-1} at 4.5 $R_\odot$ before falling to 2000 km s^{-1} at 20 $R_\odot$. In contrast, the CME is observed to decelerate from 1890 to 1699 km s^{-1} as it travels from 2.3 to 26.3 $R_\odot$.
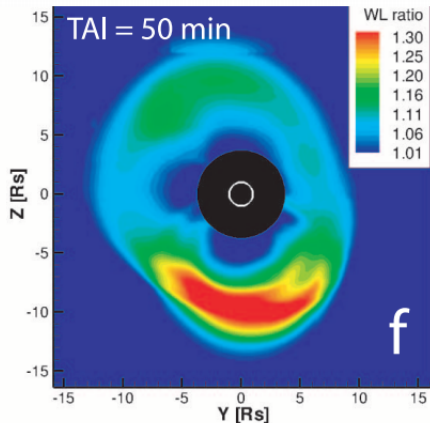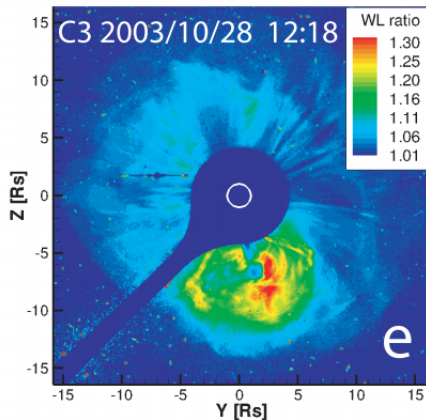
Comparison of observed (left) and simulated (right) Thomson-scattered white-light brightness
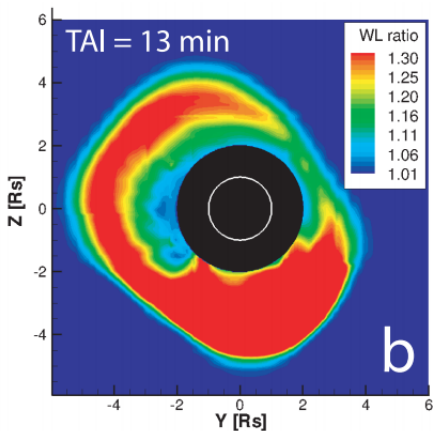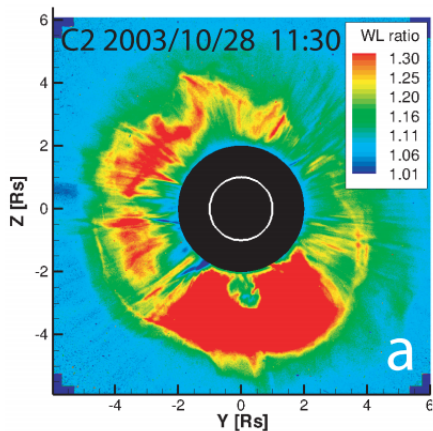
Comparison of observed (left) and simulated (right) Thomson-scattered white-light brightness
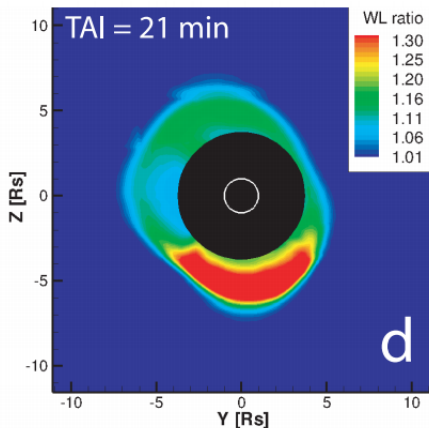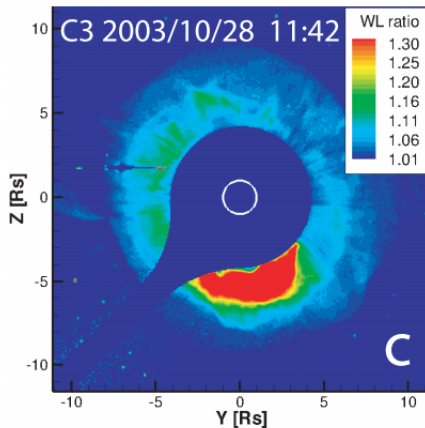
Comparison of observed (left) and simulated (right) Thomson-scattered white-light brightness

Observations

- the CME travels slower than in the model, with the observed sequence of images occurring at approximately 36, 48, and 84 minutes after initiation. The velocity in the model also larger than in observation.
- In both data and model, the color images show the total brightness divided by that of the preevent background.
- White circles show the solar limb, and filled black circles show the occulting disks.
- In all cases there is extremely good quantitative agreement in both the magnitude and spatial distribution of the observed brightness.
- brightest SE, dimmest NW ($\Longleftarrow$ position of AR, which was located at 20 below the equator on October 28)
- at 12:18 UT (the third), the observed brightness patterns is more highly structured than the model.

CME mass I

- calculated from observations by integrating the excess brightness of the K corona with the assumption that the plasma is in the plane of the sky, which sets a lower limit on CME mass. The F corona is subtracted out from the observations and does not affect the mass. We restrict this integral to the brightest portion of the CME that extends from $235°$ to $330°$ as measured from the y=0 axis. In the case of the C2 field of view (top row), this integration sector extends from 2.0 to 6.0 R_{Sun}, and for the C3 field of view (middle and bottom rows) the sector extends from 4.0 to 16.4 R_{Sun}.

- masses derived from observations are 1.5×10^{16}, 1.55×10^{16}, and 1.70×10^{16} g, respectively. The corresponding masses of the model CME are, respectively, 2.23×10^{16}, 2.16×10^{16} 4.90×10^{16} g.

- The observed masses are approximately 30% less than that of the model at times 11:30 and 11:42 UT (first two), which is consistent with the larger filling factor of the model event.

CME mass II

- The slight decrease in model CME mass found from Figure 5d (second) is the result of a greater part of the CME being obscured by the occulting disk.

- By 12:18 (the third) the CME mass is observed to increase by 13%, while the model mass (as shown in Fig. 5f) more than doubles. CME mass increases faster than what is observed because of the excess speed of the CME. For the observed event, the (excess) mass continues to increase by almost an order of magnitude, to 13.6×10^{16} g as measured with SMEI on October 29, 12:00 UT, as the CME passed the Earth.

- In the numerical model mass increase in the case of the fast CMEs as plasma is swept up as they travel from the Sun, as shown in other numerical simulations is expected.

- The mass increase seen in LASCO observations is attributed to mass entering the coronagraph field of view from below the occulter. In general, there is not yet proof of a plasma pileup in the low corona by CMEs.